

PACS 78.40.-q

## Investigation of ZnO single crystals subjected to a high uniform magnetic field in the IR spectral range

E.F. Venger<sup>1</sup>, A.I. Evtushenko<sup>2</sup>, L.Yu. Melnichuk<sup>2</sup>, O.V. Melnichuk<sup>2</sup>

<sup>1</sup>*V. Lashkaryov Institute of Semiconductor Physics, NAS of Ukraine*

*41, prospect Nauky, 03028 Kyiv, Ukraine*

*Phone: (380-44) 525-25-93; e-mail: venger@isp.kiev.ua*

<sup>2</sup>*Mykola Gogol State Pedagogic University*

*2, Kropyv'yans'kogo str., 16600 Nizhyn, Ukraine*

*E-mail: mov310@mail.ru*

**Abstract.** Based on the experimental data obtained, we performed the theoretical investigation of the external reflectance coefficients of uniaxial optically anisotropic polar ZnO single crystals subjected to the action of a high uniform magnetic field that is parallel to the crystal axis  $C$  and the surface under the condition that  $\vec{E} \perp \vec{B}$  (the Voigt configuration, Fig. 1). For the first time, we have found the regions in the external reflection spectra of ZnO single crystals, where new oscillations appear which are due to the effect of a high uniform magnetic field. A possibility of solving the direct and inverse problems in such a case is demonstrated.

**Keywords:** Voigt configuration, ZnO, reflection spectra.

Manuscript received 23.01.08; accepted for publication 07.02.08; published online 31.03.08.

### 1. Introduction

Zinc oxide ZnO is one of the binary compounds that belong to the wide class of II–VI semiconductors. It crystallizes in the wurtzite structure (space group  $C_{6v}^4$  ( $P6_3mc$ )). Zinc oxide has unique physico-chemical properties which make it potentially applicable in metallurgy, space engineering, acousto-, micro-, and optoelectronics, as well as in some other areas of science, engineering, and medicine [1]. ZnO single crystals demonstrate a great anisotropy of the properties of their phonon subsystem, while the anisotropy of their plasmon subsystem is small [2]. The spectra of external reflection from the surface of ZnO single crystals (with electron concentrations from  $10^{16}$  up to  $5 \cdot 10^{19}$   $\text{cm}^{-3}$ ) were studied experimentally in [3], and the consistent bulk parameters were obtained. In [4], the reflectance coefficient of ZnO single crystals in IR was studied for the first time with allowance made for vibrations of three coupled subsystems: electromagnetic waves, optical vibrations of the crystal lattice, and plasma oscillations of free charge carriers (for the orientations  $E \perp C$  and  $E \parallel C$ ). In [5, 6], it was shown that zinc oxide is a typical optically anisotropic semiconductor. Many its properties have been investigated. However, there are no data in

the literature on the effect of high uniform magnetic fields on the reflectance coefficient of this optically anisotropic single crystal.

The objective of this work was the investigation of the external reflectance coefficients of optically anisotropic polar ZnO single crystals subjected to a high uniform magnetic field that is parallel to the crystal axis  $C$  and the surface under the condition that  $\vec{E} \perp \vec{B}$  (the Voigt configuration, Fig. 1), as well as the determination of regions where the external reflectance coefficient varies in IR under the action of a uniform magnetic field.

### 2. Experimental

It is known that if a semiconductor is subjected to the action of a magnetic field, then a number of effects appear, in particular, the Zeeman effect, diamagnetic shifting and transitions between the Landau levels, etc. (see, e.g., [7]). A comprehensive analysis of the latter was made in [8] by using CdSe as an example. The spectral curves in a cubic magnetic semiconductor, the Cotton-Mouton effect quadratic in a magnetic field (the Voigt effect), nonreciprocal birefringence linear in a magnetic field, and the Faraday effect were investigated in [9]. It was shown that the Voigt effect is anisotropic in

cubic magnetic semiconductors. The propagation of electromagnetic waves in uniaxial semiconductors subjected to a magnetic field which is not parallel to the crystal axis was considered in [10]. It was shown, in particular, that the effect of cyclotron and plasma resonance shifting is related to their transformation to the combined cyclotron-plasma resonances. The Faraday effect in cubic and hexagonal crystals was considered in [11] (without comprehensive analysis of expressions for the Faraday rotation). We do not know about investigations of the external reflectance coefficients in uniaxial optically anisotropic single crystals subjected to a uniform magnetic field.

As an example, we consider optically anisotropic  $n$ -ZnO single crystals (with gap  $E_g \leq 3.43$  eV) obtained using the hydrothermal technique. Their optical and electrophysical parameters (determined by us in [3, 6]) are presented in Tables 1 and 2, respectively.

Here, we consider the case where  $\vec{E} \perp \vec{B}$  (Fig. 1) (the Voigt configuration), i.e., the magnetic birefringence which is as follows. A linear polarized radiation directed along a normal to the magnetic field becomes elliptically polarized after having passed a layer of an isotropic matter subjected to the magnetic field. This is due to the optical anisotropy of the matter which appears in the magnetic field and is oriented along this field. We consider the case where the magnetic field induced by the current flowing through the semiconductor is insignificant.

In the system of coordinates with the  $z$ -axis oriented along the external magnetic field  $\vec{B}$  (which lies in the  $xz$ -plane and makes an angle  $\varphi$  with the crystal axis), the components of the permittivity tensor of a ZnO single crystal are of the following form [10]:

$$\left\{ \begin{array}{l} \varepsilon_{xx} = \varepsilon_{xx}^{\infty} - \frac{\mu_{xx}\omega_0^2}{\omega^2 - \Omega^2}, \\ \varepsilon_{yy} = \varepsilon_{\perp}^{\infty} - \frac{\mu_{\perp}\omega_0^2}{\omega^2 - \Omega^2}, \\ \varepsilon_{zz} = \varepsilon_{zz}^{\infty} - \mu_{zz} \frac{\omega_0^2}{\omega^2} \left[ 1 + \frac{\Omega^2}{\omega^2 - \Omega^2} \left( 1 - \frac{\mu_{\perp}\mu_{\parallel}}{\mu_{xx}\mu_{zz}} \right) \right], \\ \varepsilon_{xz} = \varepsilon_{zx} = \varepsilon_{xx}^{\infty} - \frac{\mu_{xz}\omega_0^2}{\omega^2 - \Omega^2}, \\ \varepsilon_{xy} = \varepsilon_{yx}^* = i \frac{\omega_0^2 \Omega \sqrt{\mu_{\perp}\mu_{xx}}}{\omega(\omega^2 - \Omega^2)}, \\ \varepsilon_{yz} = \varepsilon_{zy}^* = i \frac{\omega_0^2 \Omega \mu_{xz}}{\omega(\omega^2 - \Omega^2)} \sqrt{\frac{\mu_{\perp}}{\mu_{xx}}}. \end{array} \right. \quad (1)$$

**Table 1. Parameters of the ZnO bulk.**

ZnO	$\varepsilon_0$	$\varepsilon_{\infty}$	$\nu_T, \text{cm}^{-1}$	$\nu_L, \text{cm}^{-1}$
$E \perp C$	8.1	3.95	412	591
$E \parallel C$	9.0	4.05	380	570

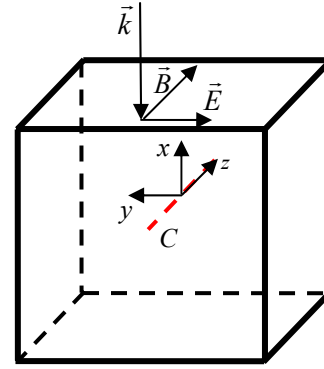


**Fig. 1.** Voigt configuration.

Here,  $\Omega = \frac{eB}{mc} \sqrt{\mu_{\perp}\mu_{xx}}$  is the cyclotron frequency, and the components of the dimensionless tensor of inverse effective mass  $\mu_{ij}$  are expressed in terms of the principal values  $\mu_{\perp}$  and  $\mu_{\parallel}$ :

$$\left\{ \begin{array}{l} \mu_{xx} = \mu_{\perp} \cos^2 \theta + \mu_{\parallel} \sin^2 \theta, \\ \mu_{yy} = \mu_{\perp}, \\ \mu_{zz} = \mu_{\perp} \sin^2 \theta + \mu_{\parallel} \cos^2 \theta, \\ \mu_{xz} = \mu_{zx} = (\mu_{\parallel} - \mu_{\perp}) \sin \theta \cos \theta, \\ \mu_{xy} = \mu_{yx} = \mu_{yz} = \mu_{zy} = 0. \end{array} \right. \quad (2)$$

where  $\theta$  is the angle between the crystal axis and the  $z$ -axis. Similar expressions exist also for the components of the high-frequency permittivity tensor of the crystal lattice  $\varepsilon_{ij}^{\infty}$ .

By solving the dispersion equation

$$\left| \varepsilon_{ij} + n^2 (s_i s_j - \delta_{ij}) \right| = 0, \quad \vec{s} = \frac{\vec{k}}{k}, \quad n = \frac{ck}{\omega}, \quad (3)$$

one obtains that an extraordinary (longitudinal-transverse) wave with  $\vec{E} \perp \vec{B}$ ,  $\vec{H} \parallel \vec{B}$  can propagate across the magnetostatic field  $\vec{E}$ . At  $\theta = 0$ , the refractive index of such a wave obeys the equation

$$n^2 = \varepsilon_{\perp}^{\infty} \frac{(\omega^2 - \omega_+^2)(\omega^2 - \omega_-^2)}{\omega^2(\omega^2 - \omega_p^2)}, \quad (4)$$

where  $\omega_{\pm}^2 = \omega_{0\perp}^2 + \frac{\Omega^2}{2} \left( 1 \pm \sqrt{1 + 4 \frac{\omega_{0\perp}^2}{\Omega^2}} \right)$  and

$$\omega_p^2 = \Omega^2 + \omega_{0\perp}^2.$$

Since  $\vec{E} \perp \vec{B}$  in electromagnetic waves, the external reflectance coefficient can be written as

$$R = \left| \frac{1-n}{1+n} \right|^2. \quad (5)$$

The frequency dependence of the permittivity in the region of plasmon-phonon interaction is [3]

**Table 2. Electrophysical parameters of ZnO single crystals grown with the use of the hydrothermal technique.**

N	Sample	$n, \text{cm}^{-3}$	$\nu_p, \text{cm}^{-1}$		$\gamma_p, \text{cm}^{-1}$		$\gamma_f, \text{cm}^{-1}$		$m_{\parallel}$	$\frac{m_{\perp}}{m_{\parallel}}$	$m_{\perp}$	$\mu_{\parallel}$	$\mu_{\perp}$
			$E \perp C$	$E \parallel C$	$E \perp C$	$E \parallel C$	$E \perp C$	$E \parallel C$					
1	ZO2-3	$9.3 \times 10^{16}$	90	100	150	170	11	11	0.21	1.23	0.258	4.76	3.88
2	ZO1-3	$6.6 \times 10^{17}$	240	250	280	260	13	13	0.23	1.13	0.260	4.35	3.85
3	ZO6-B	$2.0 \times 10^{18}$	420	480	406	350	21	21	0.22	1.18	0.260	4.55	3.85

$$\varepsilon(\nu) \equiv \varepsilon_1(\nu) + i\varepsilon_2(\nu) = \varepsilon_{\infty} + \left[ \varepsilon_{\infty} (\nu_L^2 - \nu_T^2) \right] / \left[ \nu_T^2 - \nu^2 - i\nu\gamma_f \right] - \left( \nu_p^2 \varepsilon_{\infty} \right) / \left[ \gamma(\nu + i\gamma_p) \right]. \quad (6)$$

Here,  $\varepsilon_{\infty}$  is the high-frequency permittivity;  $\nu_L, \nu_T$  the frequencies of the longitudinal and transverse optical phonons, respectively;  $\gamma_f$  the optical phonon damping coefficient;  $\nu_p$  the plasma resonance frequency; and  $\gamma_p$  the plasmon damping coefficient. Taking Eq. (6) into account, we obtain the frequency dependence of the refractive index for a low-doped ZnO single crystal (whose parameters are given in Tables 1 and 2) at different values of the magnetic field (Fig. 2). Curve 1 (Figs. 2-5) corresponds to the dependence  $R(\nu)$  without the effect of a magnetic field. It agrees with the curve  $R(\nu)$  obtained in [3] for a single-oscillator model of ZnO. Curves 2-4 (Figs. 2 and 3) correspond to the dependences  $R(\nu)$  at high (30–100 kGs) magnetic fields.

One can see from Fig. 2 that, in high magnetic fields, the number of minima and peaks of the reflectance coefficient (which shifts towards higher frequencies) increases. Table 3 presents the frequencies of the minimum and the peak at various values of the magnetic field. One can see from Fig. 2 that the resonance frequency of the minimum of the external reflectance coefficient decreases as the uniform magnetic field grows from 30 up to 100 kGs; however,  $R_{\min} \neq 0$ . In this case, the resonance frequency of the peak of the external reflectance coefficient increases; however,  $R_{\max} \neq 1$ . One should note that, in the case where  $\vec{E} \perp \vec{B}$ , no changes in the external IR reflectance spectra in the 355–1200-cm<sup>-1</sup> frequency region occur as the uniform magnetic field grows.

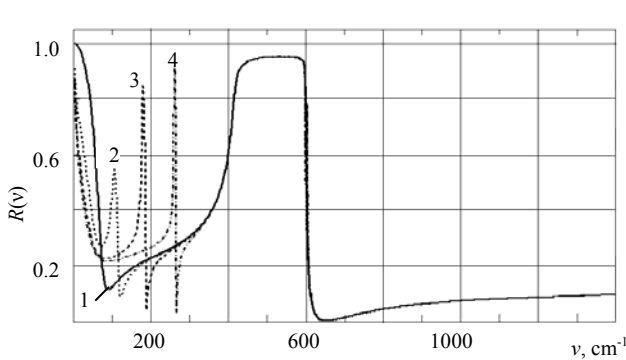


**Fig. 2.** Frequency dependence of the reflectance coefficient  $R(\nu)$  of a ZnO single crystal (sample ZO2-3) in the uniform magnetic field: 1 –  $B = 1$  Gs; 2 – 30 kGs; 3 – 65 kGs; 4 – 100 kGs.

In Fig. 3, we show the  $R(\nu)$  curves of the sample ZO6-B (for its parameters see Table 2). One can see that there is no effect of a uniform magnetic field in the 370–640- and 840–1200-cm<sup>-1</sup> frequency ranges. The biggest change of the external reflectance coefficient of a heavily doped ZnO single crystal under the action of the uniform magnetic field occurs in the 250–380-cm<sup>-1</sup> frequency range (see the inset in Fig. 3). Contrary to the previous case, some new peaks and minima were detected in the IR external reflectance spectra near 300 cm<sup>-1</sup> as the magnetic field grew. Our calculations showed, however, that their shifts towards higher IR frequencies with increase in the magnetic field strength were insignificant in this case.

Figures 4 and 5 show the  $R(\nu)$  curves for low-doped ZnO single crystals in a magnetic field of 65 kGs at various values of the optical phonon damping coefficient (the plasma frequency and the damping coefficient of optical plasmons remaining the same). One can see from Fig. 4 that, at  $\nu_p = 100$  cm<sup>-1</sup> and  $\gamma_p = 100$  cm<sup>-1</sup>, one more peak (minimum) appears in the reflection spectrum at a frequency of 180 (190) cm<sup>-1</sup> in a uniform magnetic field of 65 kGs. In the 390–600-cm<sup>-1</sup> frequency range, the reflectance coefficient decreases as the optical phonon damping coefficient grows.

Figure 5 presents the reflectance spectra of zinc oxide single crystals (the plasma frequency  $\nu_p = 500$  cm<sup>-1</sup> and the plasmon damping coefficient  $\gamma_p = 500$  cm<sup>-1</sup>). One can see from the inset that, in the 250–380-cm<sup>-1</sup> frequency range,  $R_{\min}(\nu)$  increases from 0.295 up to 0.36, as the phonon damping coefficient  $\gamma_f$  grows from 11 up to 30 cm<sup>-1</sup>. At the same time,  $R_{\max}(\nu)$  decreases from 0.925 down to 0.875 in the 400–570-cm<sup>-1</sup> frequency range.

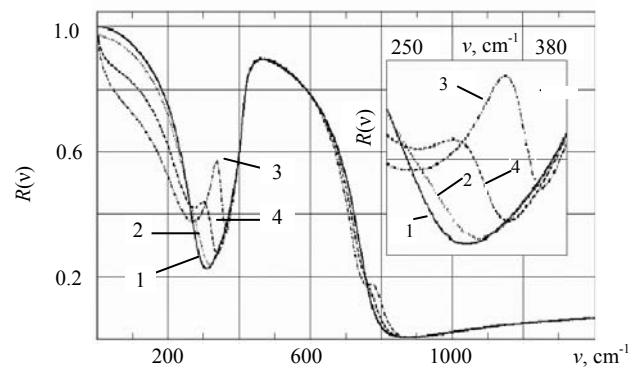


**Fig. 3.** As in Fig. 2, but for the sample ZO6-B. Inset: the same in the 250–380-cm<sup>-1</sup> frequency range.

**Table 3. Frequencies of minima and peaks of the external reflectance coefficient of a low-doped ZnO crystal at various magnetic field strengths.**

Curve number in Fig. 2	$B$ , kGs	$\nu_{\min}$ , $\text{cm}^{-1}$	$\nu_{\max}$ , $\text{cm}^{-1}$
2	30	89	98
3	65	115	163
4	100	172	236

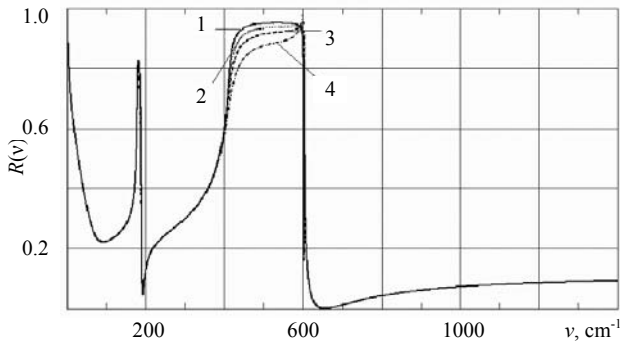


**Fig. 4.** Reflectance coefficient  $R(\nu)$  of a ZnO single crystal versus the frequency at  $\nu_p = 100 \text{ cm}^{-1}$  and  $\gamma_p = 100 \text{ cm}^{-1}$ ,  $B = 65 \text{ kGs}$ ;  $\gamma_f = 11$  (1), 15 (2), 20 (3), and 30 (4)  $\text{cm}^{-1}$ .

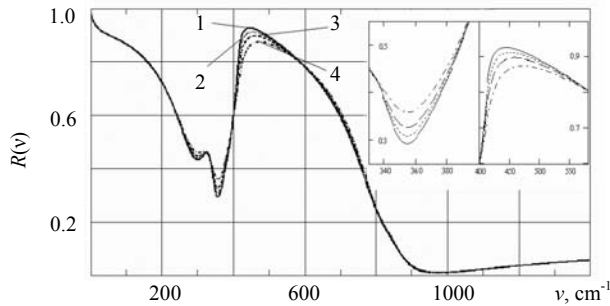


**Fig. 5.** As in Fig. 4, but at  $\nu_p = 500 \text{ cm}^{-1}$  and  $\gamma_p = 500 \text{ cm}^{-1}$ .

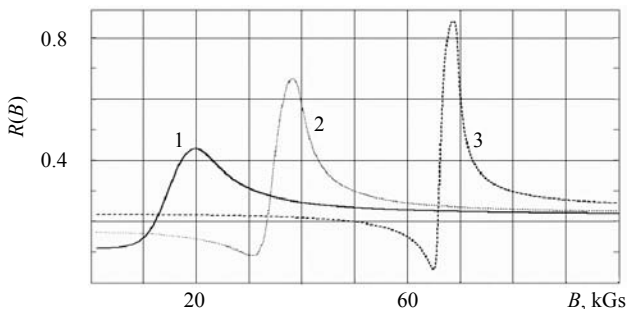


**Fig. 6.** Dependence of the minima of reflectance coefficient of ZnO single crystal (sample ZO2-3) on uniform external magnetic field at frequencies  $\nu = 88$  (1), 119 (2) and 186  $\text{cm}^{-1}$  (3).

By analyzing the obtained external reflectance spectra (Figs. 2-5), one can conclude that the biggest effect of a uniform magnetic field on the reflectance

coefficient of an optically anisotropic ZnO single crystal occurs in a low-doped sample (Fig. 2).

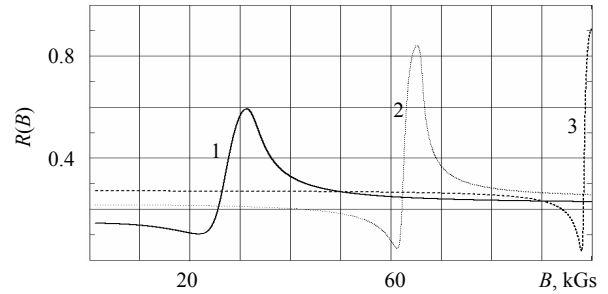


**Fig. 7.** As in Fig. 6, but at the frequencies  $\nu = 104$  (1), 177 (2), and 259 (3)  $\text{cm}^{-1}$ .

Figures 6 and 7 show the dependence of the reflectance coefficient on the uniform magnetic field strength measured at the frequencies that correspond to the minima and the peaks of the  $R(\nu)$  curves of a low-doped ZnO single crystal (sample ZO2-3) presented in Fig. 2 (curves 2-4).

### 3. Conclusions

It follows from the results of our investigations that if ZnO single crystals are subjected to a high uniform magnetic field ( $B = 1\text{--}100 \text{ kGs}$ ), some anomalies of the external reflection coefficient appear in their IR reflection spectra.

One of the considerable results of our work is that, using an optically anisotropic ZnO single crystal as an example, the spectral regions, where the novel oscillations appear in the external reflection spectra under the action of a high uniform magnetic field in the Voigt configuration ( $\vec{E} \perp \vec{B}$ ), are first discovered. This fact seems to be of interest for the establishment of fixed points on the magnetic field scale. In addition, we have detected for the first time that the most essential changes in the IR reflection spectra (the appearance of additional minima and peaks) occur in low-doped single crystals subjected to high uniform magnetic fields. The dependences of the reflectance coefficient and the frequencies of spectral extrema on the strength of a uniform magnetic field are determined. This makes it possible to solve both the direct problem (the investigation of the physical and chemical properties of a semiconductor subjected to the magnetic field of a given strength) and the inverse problem (by getting the information on the external uniform magnetic field from the known optical and electrophysical parameters of a semiconductor).

### References

1. I.P. Kuz'mina, V.A. Nikitenko, *Zinc Oxide. Preparation and Optical Properties*. Nauka, Moscow, 1984 (in Russian).

2. E.F. Venger, A.V. Melnichuk, L.Ju. Melnichuk, Ju.A. Pasechnik // *Phys. status solidi (b)* **188**(2), p. 823 (1995).
3. A.V. Melnichuk, L.Yu. Melnichuk, Yu.A. Pasechnik // *Fiz. Tverd. Tela* **36**(9), p. 2624 (1994) (in Russian).
4. E.F. Venger, L.Yu. Melnichuk, O.V. Melnichuk, Yu.A. Pasichnyk // *Ukr. Fizychny Zhurnal* **45**(8), p. 976 (2000) (in Ukrainian).
5. R.J. Collins, D.A. Kleinman // *J. Phys. Chem. Sol.* **11**(3-4), p. 190 (1959).
6. E.F. Venger, O.V. Melnichuk, Yu.A. Pasichnyk, *Residual Rays Spectroscopy*. Naukova Dumka, Kyiv, 2001 (in Ukrainian).
7. F.F. Sizov, Yu.I. Ukhanov, *Magneto-optical Faraday and Voigt Effects as Applied to Semiconductors*. Naukova Dumka, Kiev, 1979 (in Russian).
8. A.B. Kapustina, B.V. Petrov, A.V. Rodina, R.P. Seisyan // *Fizika tverdogo tela* **42**(7), p. 1207-1217 (2000) (in Russian).
9. B.B. Krichevtsov, H.-J. Weber // *Fizika tverdogo tela* **46**(3), p. 488-494 (2000) (in Russian).
10. L.E. Gurevich, R.G. Tarkhanyan // *Fizika Techn. Poluprov.* **6**(4), p. 703 (1972) (in Russian).
11. L.E. Gurevich, I.P. Ipatova // *Zhurnal Eksperim. Teor. Fiziki* **37**(5), p. 1324 (1959) (in Russian).